JOURNAL OF VIROLOGY, Mar. 2010, p. 2453–2465 Vol. 84, No. 5
0022-538X/10/$12.00 doi:10.1128/JVI.01543-09

Induction of Protective Immunity against Murine Gammaherpesvirus 68 Infection in the Absence of Viral Latency[▽]

Qingmei Jia,[1] Michael L. Freeman,[4] Eric J. Yager,[4] Ian McHardy,[1] Leming Tong,[1] DeeAnn Martinez-Guzman,[2] Tammy Rickabaugh,[1] Seungmin Hwang,[1] Marcia A. Blackman,[4] Ren Sun,[1] and Ting-Ting Wu[1,3]*

Department of Molecular and Medical Pharmacology, School of Medicine,[1] Molecular Biology Institute,[2] and Dental Research Institute, School of Dentistry,[3] University of California at Los Angeles, Los Angeles, California 90095, and The Trudeau Institute, Saranac Lake, New York 12983[4]

Received 26 July 2009/Accepted 8 December 2009

Human gammaherpesviruses, Epstein-Barr virus, and human herpesvirus 8/Kaposi's sarcoma-associated herpesvirus are important pathogens associated with diseases, including lymphomas and other malignancies. Murine gammaherpesvirus 68 (MHV-68) is used as an experimental model system to study the host immune control of infection and explore novel vaccine strategies based on latency-deficient live viruses. We studied the properties and the potential of a recombinant MHV-68 (AC-RTA) in which the genes required for persistent infection were replaced by a constitutively expressed viral transcription activator, RTA, which dictates the virus to lytic replication. After intranasal infection of mice, replication of AC-RTA in the lung was attenuated, and no AC-RTA virus or viral DNA was detected in the isolated splenocytes, indicating a lack of latency in the spleen. Infection of the AC-RTA virus elicited both cellular immune responses and virus-specific IgG at a level comparable to that elicited by infection of the wild-type virus. Importantly, vaccination of AC-RTA was able to protect mice against subsequent challenge by the wild-type MHV-68. AC-RTA provides a vaccine strategy for preventing infection of human gammaherpesviruses. Furthermore, our results suggest that immunity to the major latent antigens is not required for protection.

Human gammaherpesviruses, Epstein-Barr virus (EBV)/human herpesvirus 4 (HHV-4), and Kaposi's sarcoma-associated herpesvirus (KSHV)/HHV-8 are significant pathogens of human diseases (32). EBV is associated with Burkitt's lymphoma, nasopharyngeal carcinoma, Hodgkin's disease, and lymphoproliferative diseases in immunodeficient patients (35). HHV-8 is associated with Kaposi's sarcoma, primary effusion lymphoma, and multicentric Castleman's disease (9, 11, 12, 53). The life cycle of gammaherpesviruses involves two distinctive stages, lytic and latent infection, both of which play critical roles in gammaherpesvirus-related pathogenesis. The balance between latency and lytic replication *in vivo* determines the pathogenic outcome of the virus, and latently infected cells have the potential to become transformed. Therefore, preventing latent infection has been a critical task in the field of gammaherpesvirus research. However, due to the strict host specificity of human gammaherpesviruses, studies on the vaccine strategies against human gammaherpesvirus infection have been limited.

Murine gammaherpesvirus 68 (MHV-68), another member of the *Gammaherpesvirinae* subfamily, has been used as a model system to study the virus-host interactions during infection of gammaherpesviruses. MHV-68 is a naturally occurring pathogen among wild rodents (3, 5, 6, 44), and its viral genome has been shown to be closely related to EBV and KSHV (16, 17, 40, 68). In contrast to EBV and KSHV/HHV-8, MHV-68 robustly infects a variety of cell lines as well as laboratory mice. Therefore, genetic mutagenesis has been extensively conducted on the MHV-68 genome to elucidate the function of individual viral genes. Furthermore, MHV-68 has provided a tractable model to examine the efficacy of various vaccine strategies for gammaherpesviruses. Peptide and subunit vaccination targeting lytic and latency-associated viral proteins reduces acute infection in the lungs and peak latency in the spleens of laboratory mice (37, 46, 55, 57, 65, 73). Similar effects have also been demonstrated for a vaccine based on heat-inactivated MHV-68 (1). These vaccine strategies can reduce acute MHV-68 infection but do not affect the establishment of long-term latency, which predisposes the host to viral tumorigenesis.

A vaccine based on a live and attenuated virus allows for the presentation of the full repertoire of viral antigens in the context of active replication and thus effectively elicits both humoral and cellular immunity. However, the primary concern of using a live virus as a vaccine for gammaherpesviruses is the tumorigenicity associated with the establishment of latency. Several latency-deficient live MHV-68 viruses have been constructed and proven to be effective to reduce not only lytic but also latent infections from a challenge virus (7, 22, 48, 63). One strategy to create a latency-deficient phenotype is constitutively overexpressing a viral transcription activator (RTA) to keep the virus constantly in a lytic cycle. RTA is an immediate-early protein conserved among gammaherpesviruses. It has been shown that HHV-8 RTA and its homologue in MHV-68 are necessary and sufficient to reactivate their respective viruses in latently infected cells (15, 24, 38, 39, 47, 59, 74, 75). MHV-68 RTA has been shown to play an important role in

* Corresponding author. Mailing address: 650 Charles E. Young Drive, CHS 23-120, University of California at Los Angeles, Los Angeles, CA 90095. Phone: (310) 267-2218. Fax: (310) 794-5123. E-mail: twu@mednet.ucla.edu.

▽ Published ahead of print on 16 December 2009.

controlling latency *in vivo* (7, 48). A recombinant MHV-68 (C-RTA) virus was previously constructed in our laboratory with an ectopic RTA expression cassette driven by a cytomegalovirus (CMV) immediate-early promoter inserted at the left end of the viral genome (48). We have shown that C-RTA is deficient in establishing latency and has the capacity to protect mice against a wild-type (WT) MHV-68 challenge infection. However, latency establishment was detected in a portion of mice infected with C-RTA virus due to the spontaneous loss of the RTA expression cassette. Others have also generated a recombinant MHV-68 virus with enhanced transcription of open reading frame 50 (ORF50); similar to our C-RTA study, this virus was attenuated in latency establishment and afforded protection from a subsequent WT virus infection (7). Another strategy to construct a latency-deficient live virus is eliminating a latency-associated gene ORF73 to abolish latency establishment and maintenance of the virus. MHV-68 ORF73 encodes a homologue of the KSHV latency-associated nuclear antigen (LANA). KSHV LANA has been shown to be required for maintenance of viral episomes during latency (2) and capable of inhibiting lytic replication (34, 36). In MHV-68, disruption of ORF73 compromised the ability of MHV-68 to establish latency in the spleen (23, 45). A ORF73-null virus has been shown to protect mice from a challenge infection of the WT MHV-68 (22).

In order to understand the mechanisms of establishment and maintenance of gammaherpesvirus latency, efforts have been made to identify viral genes that are expressed during latency (14, 18, 19, 26, 32, 41, 49, 51, 69). It has been shown that a region located at the right end of the viral genomes is transcribed during latency. For example, this latency locus in KSHV contains ORFs 71 to 73. In addition to analysis of latency-associated transcripts, studies using MHV-68 mouse infection model have revealed that several gene products, including ORF73 play important roles in latency (10, 13, 23, 25, 30, 45, 56, 67). Among them, ORF72 and a viral bcl-2 homologue, M11, are located adjacent to ORF73 on the MHV-68 genome, and their homologues are also encoded by HHV-8/KSHV. The gene product of ORF72 is a viral cyclin (v-cyclin) and has been shown to play a role in reactivation from latency (27, 67). Moreover, the ability of v-cyclin to promote cell cycle progression implicates that v-cyclin may contribute to virus-associated tumorigenesis (61, 66). M11 encoding an antiapoptotic oncogenic protein v-bcl-2 is actively transcribed in lytically infected fibroblast cells and latently infected tissues (42, 50, 69). M11 is not required for MHV-68 lytic replication but may be involved in latency establishment and ex vivo reactivation (13, 25). More recently, M11 has been shown to inhibit Beclin-mediated autophagy (33). Based on the above-mentioned functions of RTA and the latency-associated proteins, we reasoned that a combination of overexpression of RTA and deletion of the major latency locus (including M11, ORF72, and ORF73) could further reduce the capacity of the virus to establish and maintain latency and thus increase the safety of the virus as a vaccine. Such a recombinant virus was constructed and studied for its replication kinetics *in vivo* by both conventional experimental approaches and noninvasive bioluminescence imaging. We also demonstrated the efficacy of the recombinant virus in preventing lytic and latent infection from the challenge of WT MHV-68. Since RTA and ORF72, M11 and ORF73 are conserved among other gammaherpesviruses, our results have significant implications for the development of live attenuated vaccine viruses for human gammaherpesviruses.

MATERIALS AND METHODS

Viruses, cells, and plaque assays. WT MHV-68 was originally obtained from the American Type Culture Collection (ATCC; VR1465). The working stocks of WT and recombinant MHV-68 (C-RTA and AC-RTA) viruses were generated by infecting BHK-21 cells (a baby hamster kidney fibroblast cell line; ATCC CCL-10) at a multiplicity of infection (MOI) of 0.05 PFU/cell. BHK-21 cells were cultured in complete Dulbecco modified Eagle medium (DMEM) containing 10% fetal bovine serum and supplemented with penicillin and streptomycin. Virus titers were determined by plaque assays that were performed on monolayers of BHK-21 cells overlaid with 1% methylcellulose as described previously (75).

Molecular cloning. The AC-RTA bacterial artificial chromosome (BAC) plasmid was constructed by using homologous recombination in a BAC system as described previously (31). To construct the suicide shuttle plasmid for the generation of AC-RTA BAC, a 1.5-kb fragment containing an insertion of triple restriction enzyme sites of StuI-SpeI-SnaBI located between nucleotides (nt) 102425 and 104869 of the viral genome and ca. 750-bp nucleotides on each side of the insertion homologous to the viral genome was generated by a two-step PCR. First, the upstream DNA fragment of nt 102425 was amplified by using the primers 5′-GAT GAC *CAT ATG* CAC CTG ATT *GGC TAG CAC*-3′ and 5′-TCA GAT A*AG GCC T*GG *ACT AGT* GC*T ACG TA*A TTT GCC CTT TCC TCG TTG-3′. The downstream DNA fragment of nt 104869 was amplified with the primers 5′-GGG CAA AT*T ACG TA*G C*AC TAG TCC AGG CCT* TAT CTG AAA GAG ATA AAG-3′ and 5′-GCC AA*G TCG AC*C ATA TAA ACG CAC CAT GTG-3′. The restrictions sites in the primers are italicized and sequences derived from the MHV-68 genome are underlined. The 1.5-kb PCR fragment was then generated by using the upstream and downstream fragments as the templates for PCR amplification with the primers 5′-GAT GAC *CAT ATG* CAC CTG ATT GGC TAG CAC-3′ and 5′-GCC AA*G TCG AC*C ATA TAA ACG CAC CAT GTG-3′. The resulting PCR fragment was then cloned into the SphI-SmaI sites of pSVL to construct pSVL/LAL. An ectopic FLAG-tagged RTA expression cassette driven by a β-actin CMV immediate-early hybrid promoter/enhancer was inserted into the StuI-SpeI-SnaBI sites of pSVL/LAL with either a right or a left orientation. The ectopic FLAG-RTA expression cassette flanked by the MHV-68 sequences was then subcloned into pGS284 by using NheI and SmaI sites to construct the shuttle plasmid. The resulting plasmid, pGS284/LAL/AC-RTA, was screened by colony PCR to amplify nucleotides encoding the ectopic RTA. The positive clones identified by PCR screening were further confirmed by restriction enzyme digestion.

Construction of AC-RTA and M3-FL/AC-RTA BAC plasmids. The AC-RTA BAC plasmid was generated by allelic exchange in *Escherichia coli* using the donor bacterial strain carrying the shuttle plasmid, pGS284/LAL/AC-RTA, and the recipient strain harboring the WT MHV-68 BAC plasmid, as described by Smith and Enquist (52), with modifications. The deletion of the nucleotides encoding ORF72, M11, and ORF73 and the insertion of an ectopic RTA expression cassette were screened by colony PCR, and the resultant BAC plasmids were confirmed by Southern blot analysis. Four clones with left and two clones with right orientations of the ectopic RTA expression cassette were selected for further analyses.

M3-FL/AC-RTA was constructed by allelic exchange using the donor strain with a shuttle plasmid that contained a firefly luciferase expression cassette inserted at the left end of the MHV-68 genome and the recipient strain harboring the AC-RTA BAC plasmid (clone 95). The firefly luciferase is driven by the M3 promoter, which is an early-late viral promoter and highly responsive to RTA induction (42). The resultant M3-FL/AC-RTA BAC plasmid contained the luciferase expression cassette inserted into the left end of the viral genome (between nt 746 and nt 747) without disrupting any known ORFs. The M3-FL/AC-RTA BAC plasmid DNA was confirmed by Southern blot analysis.

Generation of AC-RTA and M3-FL/AC-RTA viruses. The AC-RTA BAC viruses were reconstituted by transfection of BHK-21 cells with the AC-RTA(BAC) plasmids. All four clones were used to reconstitute the AC-RTA(BAC) viruses. Based on the similarity of the growth kinetics of these clones, clone 95 with a left orientation of the ectopic RTA expression cassette was chosen to prepare the working virus stock. For *in vivo* studies, the BAC sequence insertion flanked with the loxP sites was removed by cotransfection of the AC-RTA BAC plasmid (clone 95) with a Cre-recombinase expression vector. Removal of the

BAC sequence was confirmed by PCR. Similarly, M3-FL/AC-RTA viruses were reconstituted by transfection of BHK-21 cells with the M3-FL/AC-RTA BAC plasmid, together with a Cre-recombinase expression vector. The working virus stock was prepared in BHK-21 cells with an MOI of 0.05.

DNA extraction, Southern blots, and Western blots. The BAC plasmid DNA was isolated by using a Qiagen Plasmid Midi kit (Qiagen, Inc., Valencia, CA) according to the manufacturer's modified protocol. Southern blot analysis was performed as described previously (31). Briefly, the DNA digested with the restriction enzymes was run on 1% agarose gel, transferred onto a nylon membrane, and hybridized with a probe. The membrane was then scanned with a Storm imaging system (Molecular Dynamics) to detect the signals. For Western blots, the total proteins were harvested at 1 day postinfection and separated on a 10% polyacrylamide gel. The proteins were then transferred onto a nitrocellulose membrane and probed with either rabbit polyclonal antibody to ORF26 (1:500) or monoclonal antibody to the FLAG-tag. Anti-rabbit or anti-mouse immunoglobulin G (IgG) conjugated with horseradish peroxidase (Amersham Pharmacia Biotech) was used as the secondary antibody. The proteins were detected by chemiluminescence detection (ECL Plus System; Amersham Pharmacia Biotech), and the signals were detected by using a Storm imaging system (Molecular Dynamics).

Viral growth curves. The replication kinetics of WT, C-RTA, and AC-RTA were assayed in BHK-21 cells. The cells were incubated with viral inoculums at an MOI of 5 (for single step) or 0.01 (for multiple step) for 1 h at 37°C. After 1 h of incubation, the inocula were removed, the cells were washed three times with phosphate-buffered saline (PBS), and fresh medium was added to the culture. The whole culture (including cells and supernatant) was harvested at various times postinfection and subjected to three rounds of freezing and thawing. The lysates were cleared by low-speed centrifugation to remove cell debris, and then the supernatants were used for plaque assays.

Reverse transcription-PCR and quantitative PCR. Total cellular RNA was isolated from infected cells by using Tri-Reagent (MRC, Cincinnati, OH). For reverse transcription-PCR, cDNA was synthesized by using total RNA (1 μg) as the template and oligo(dT) as the primer. cDNA was then amplified with primers to ORF31 (5′-CCG ATG CAT GTG ATT GCG CTC TGT TTG-3′ and 5′-GGT TGG CAT GCG TTG GCA TAG ATT GAC-3′), ORF72 (5′-TGG CAA CGA GGA AAG GGC A-3′ and 5′-TAC ACC TGC GAC CTC CAT G-3′), ORF M11 (5′-TGT TGT GCG TGC GCA GCT A-3′ and 5′-TTC GCC AGG GCA TGC AAC A-3′), ORF73 (5′-GAG ACC CTT GTC CCT GTT G-3′ and 5′-CAC TTG ACC CAC ACC CTT C-3′), and ORF74 (5′-TCT CGG ATC CCA CGA TGC TTG TCC TGC GGG-3′ and 5′-TCT CCT CGA GGA GAT TAG GAG CTT AGT CTA C-3′), respectively. The nucleotides sequences from the MHV-68 viral genome are underlined in the primers. To measure the levels of viral genomes, total DNA was extracted from infected BHK-21 cells or splenocytes by using a DNeasy tissue kit (Qiagen, Valencia, CA) according to the manufacturer's instructions. For quantitative PCR, DNA was amplified by using primers and probe to the MHV-68 ORF65 and TaqMan Universal PCR Master Mix (Applied Biosystems, CA) as previously described (48). Amplification and detection were performed by using an Opticon monitor (MJ Research, Inc.). Negative controls (no template) were included for each reaction, and 150 ng of genomic DNA was analyzed in duplicates for each sample. A standard curve was obtained by measuring 1 to 10^7 copies of a BAC containing the MHV-68 genome on a background of 150 ng of uninfected splenocyte DNA. The confident detection limit was 10 copies/150 ng of genomic DNA.

MHV-68 DNA array analysis. BHK-21 cells were infected with the EGFP/MHV-68 or AC-RTA virus at an MOI of 2. At different time points postinfection, RNA was isolated by using Tri-Reagent. DNA array analysis was performed as described previously (42). Briefly, total RNA (2 μg) was used in a reverse transcription reaction primed with oligo(dT) in the presence of [α-^{32}P]dATP using a Strip-EZ kit (Ambion, Austin, TX). The arrays were prehybridized for 5 h before being incubated with the labeled cDNA for overnight at 65°C. The arrays were washed, and the signal intensity was quantitated by using a Storm imaging system with ImageQuant software (Molecular Dynamics).

Mice, virus titer, reactivation. The animal studies described here were approved by the Animal Research Committee at University of California at Los Angeles. Female BALB/c mice (Charles River Laboratories, Wilmington, MA), 5 to 8 weeks of age, were infected intranasally with 500 PFU of each virus in 20 μl of DMEM. For the vaccination studies shown in Fig. 7, 5- to 8-week-old female BALB/c mice were intranasally immunized with 500 PFU of either C-RTA or AC-RTA. The mock-vaccinated control mice were intranasally administered with DMEM. At 3 months after vaccination, the mice were challenged by intranasal inoculation of 500 PFU of WT. The virus titers in the lung and viral reactivation from splenocytes were measured as described previously (48). Briefly, the lung was homogenized in 1 ml of DMEM, and the virus titers of the lung homogenates were determined by three independent plaque assays. For infectious center assays, serial numbers of splenocytes were laid onto BHK-21 cells and after 6 days BHK-21 cells were fixed to determine the numbers of plaques. The plaques referred to as infectious centers arise as a result of the virus reactivating from latency. For ex vivo limiting dilution assays, 2×10^3/well of BHK-21 cells were seeded in 96-well plates. Serial twofold dilutions of splenocytes, starting with 10^6 cells/well were plated onto BHK-21 cells with 24 wells per dilution. After 7 days, each well was scored for cytopathic effects, and the percentage of cytopathic effects per 24 wells was determined per dilution.

Noninvasive imaging. *In vivo* bioluminescence imaging was conducted by using an optical IVIS system (Xenogen Corp., Alameda, CA). Female BALB/c mice were infected intranasally with 5×10^5 PFU of M3-FL/MHV-68 or M3-FL/AC-RTA. At the indicated times postinfection, the mice were administered intraperitoneally with 200 μg of D-luciferin (Xenogen Corp.), which was used for assaying firefly luciferase enzymatic activity. The firefly luciferase catalyzes D-luciferin to produce oxyluciferin in the presence of oxygen and cofactors emitting photons that can be detected by a charge-coupled device (CCD) camera at 562 nm. The mice were then transferred to the IVIS system, and imaging of the reporter protein was performed multiple times during 5 to 30 min after administration of D-luciferin.

ELISA. Nunc Maxisorp plates were incubated with purified MHV-68 virions disrupted by 0.05% Triton X-100 at a concentration of 5 μg/ml for overnight at 4°C. The plates were washed several times with PBS containing 0.05% Tween and blocked with 1% bovine serum albumin in PBS for 1 h at room temperature. Serial fivefold dilutions of sera, starting from 1:100, were added to the coated plates and incubated for 1 h at room temperature. After several washes, virus-specific antibody was detected by adding horseradish peroxidase (HRP)-conjugated anti-mouse IgG antibody (GE Healthcare Bio-Sciences Corp., Piscataway, NJ) and orthophenylenediamine (Sigma) as the substrate for HRP. The optical absorbance at 405 nm was read by an enzyme-linked immunosorbent assay (ELISA) reader. The virus-specific antibody titer was defined as the highest dilution that gives a reading above the average of three 1/50 normal mouse serum samples included in the same plate. For each plate, a standard immune serum was included to compare the titers obtained from different plates.

Flow cytometry analysis. Tetramer staining was performed as previously described (65). Briefly, lungs and spleens were harvested from infected mice, and lymphocyte populations were prepared. Spleen homogenates were enriched for T cells by panning with goat anti-mouse IgG (Jackson Immunoresearch). Cells were stained with allophycocyanin-conjugated D^b/$ORF6_{487-495}$ or K^d/$M2_{91-99}$ tetramers and fluorescently labeled anti-CD8 antibodies. For intracellular gamma interferon (IFN-γ) staining, T cells were stimulated for 5 h ex vivo with $M2_{91-99}$ peptide-pulsed congenic (Thy1.1) splenocytes in the presence of brefeldin A and then permeabilized and stained for intracellular accumulation of IFN-γ by using a Cytofix/Cytoperm kit (BD Biosciences). All major histocompatibility complex class I-peptide tetramers were generated by the Trudeau Institute Molecular Biology Core. Monoclonal antibodies specific for CD8 (clone 53-6.7) and IFN-γ (clone XMG1.2) were purchased from eBiosciences (San Diego, CA). All data were collected on a FACSCanto II flow cytometer (BD Biosciences) and analyzed by using FlowJo software (Tree Star).

RESULTS

Disruption of latency-associated genes and insertion of an ectopic copy of RTA in an MHV-68 (BAC) vector. To eliminate the capacity of MHV-68 to establish latency, we chose to replace a cluster of latency-associated genes, including ORF72, M11, and ORF73, with an ectopic copy of RTA by using the BAC system as described in Materials and Methods. The genomic structure of the resulting BAC DNA, MHV-68/ΔLAL/AC-RTA (AC-RTA), was analyzed by Southern blot with a probe hybridized to the regions flanking the deleted ORFs. It was predicted that in the BamHI digestion the probe would detect a single fragment of 5.2 kb from the WT BAC DNA, whereas it would detect two fragments of 1.7 and 5.1 kb from the AC-RTA BAC DNA. In the digestion of NsiI, two DNA fragments of 1.3 and 4.7 kb would be detected from WT BAC DNA, whereas fragments of 1.1 and 6.4 kb would be detected from AC-RTA BAC DNA (Fig. 1A). Four clones of AC-RTA were obtained, and their BAC DNAs were analyzed.

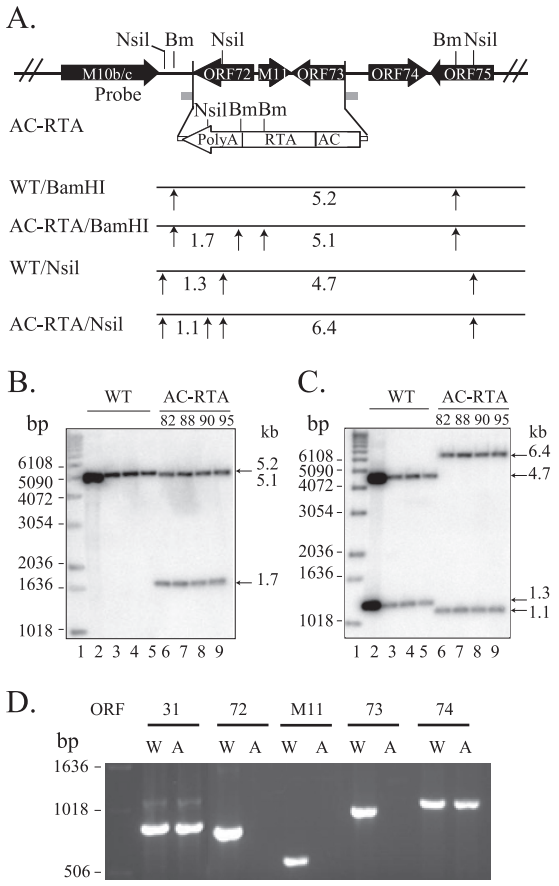

FIG. 1. Construction and confirmation of the AC-RTA virus. (A) Schematic representation of the structure of the AC-RTA genome. Shown on the top is the right end of the viral genome, including latency-associated and adjacent ORFs, represented by the solid black boxes with orientations indicated. The restriction enzyme sites of BamHI (Bm) and NsiI are indicated by solid lines and arrows. The open box represents the expression cassette of FLAG-tagged RTA driven by the human β-actin/CMV hybrid promoter/enhancer (AC) with left-orientation. In the AC-RTA virus, the region from ORF72 to ORF73 (nt 102425 and 104869) is replaced by the FLAG-tagged RTA expression cassette. The regions where the probe is derived for Southern blot analysis are shown as gray boxes. Also shown are the expected sizes of the DNA fragments resulted from restriction digestions of the WT or recombinant AC-RTA BAC plasmid DNA detected by the probe. (B, C) Southern blot analysis of the BAC plasmid DNAs digested with BamHI (B) or NsiI (C). The arrows on the right of the panels indicate the expected DNA fragments from the digestions. Seven clones (lanes 3 to 9) were included for analysis and four of them (lines 6 to 9) generated the expected fragments from the digestion of the AC-RTA BAC plasmid. (D) Reverse transcription-PCR analysis of WT and AC-RTA transcripts. RNA was isolated from BHK-21 cells infected with either the WT or AC-RTA virus and used for cDNA synthesis with oligo(dT) as a primer. The cDNA products were analyzed by PCR using primers amplifying the region of ORF31, ORF72, M11, ORF73, or ORF74.

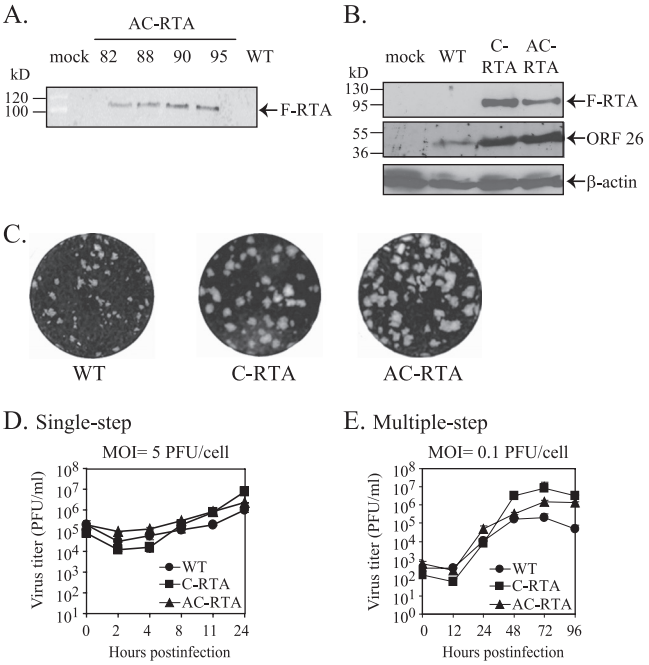

FIG. 2. Protein expression and *in vitro* replication of the AC-RTA virus. (A) Expression of the FLAG-tagged RTA by AC-RTA. BHK-21 cells were infected with four individual clones of AC-RTA. Cell lysate was harvested at 24 h postinfection to examine FLAG-tagged RTA (F-RTA) by Western blot analyses with anti-FLAG monoclonal antibody. (B) Protein expression of AC-RTA. Cells were infected with either WT, C-RTA, or AC-RTA at an MOI of 1, and the lysates were harvested at 24 h postinfection for Western blot analyses with the mouse anti-FLAG antibody (top panel) and anti-β-actin antibody (bottom panel). The membrane was then stripped and reprobed with the rabbit polyclonal anti-ORF26 antibody (middle). The sizes of protein markers are indicated on the left of the panels. (C) Plaque morphology of WT, C-RTA, and AC-RTA. Each image represents one well of a plaque assay performed on BHK-21 cells with similar titers of the viruses. (D and E) Single- and multiple-step growth curves of WT, C-RTA, and AC-RTA. BHK-21 cells were infected with individual viruses at an MOI of 5 (D) or 0.1 (E). The whole culture (supernatant and cells) was harvested at the indicated times postinfection for measuring the virus titers by plaque assays.

Digestion of these clones with either BamHI or NsiI yielded the expected patterns (Fig. 1B and C). The BAC DNAs of these clones were then transfected into BHK-21 cells to reconstitute the AC-RTA viruses. To further confirm the removal of ORF72, M11, and ORF73 from the genome of AC-RTA, we examined viral gene expression by reverse transcription-PCR analysis on RNAs isolated from cells infected with either WT or AC-RTA. The PCR products are expected to be 942, 797, 566, 999, and 1,021 bp for ORF31, ORF72, M11, ORF73, and ORF74, respectively. As shown in Fig. 1D, ORF72, M11, and ORF73 were not expressed from the AC-RTA virus, whereas the expression of ORF31 and ORF74 was detected.

Simultaneous deletion of three latency-associated genes and insertion of an ectopic copy of RTA do not compromise *in vitro* viral replication kinetics. After obtaining the AC-RTA viruses, we examined whether the ectopic RTA is expressed by Western blot analyses of the cell lysates using an antibody against the FLAG tag. As shown in Fig. 2A, all four clones of AC-RTA expressed FLAG-tagged RTA (Fig. 2A), and clone 95 was chosen for further studies. We also examined the expression of a capsid protein, ORF26, and found that the ORF26 expression was upregulated in cells infected with the AC-RTA virus compared to WT (Fig. 2B). This increase in the ORF26 expression was also observed in cells infected with C-RTA. Furthermore, the plaques formed by the AC-RTA virus were significantly larger than those formed by WT (Fig. 2C) and

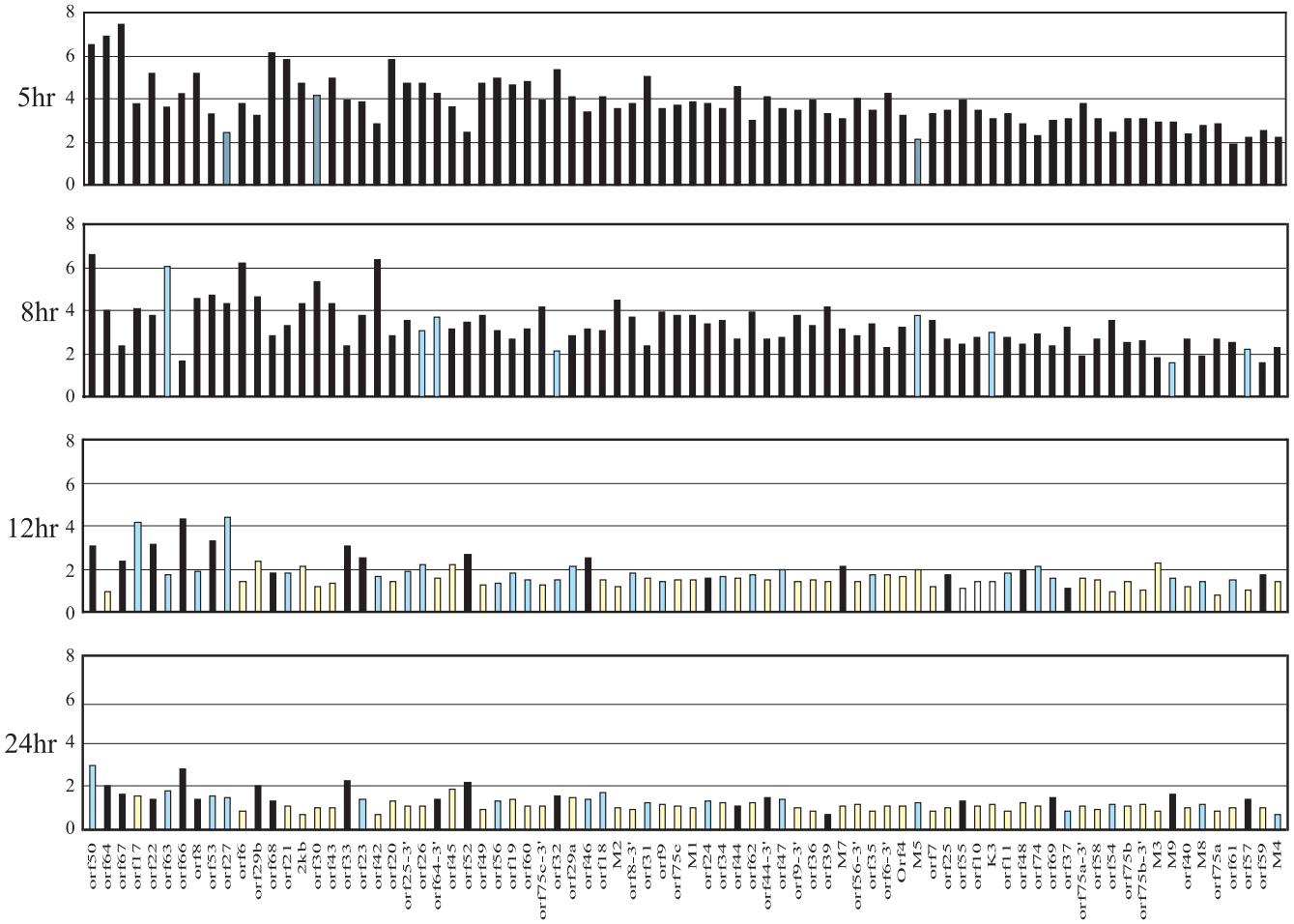

FIG. 3. Comparison of viral gene expression profiles. RNA was harvested from BHK-21 cells infected with either AC-RTA or EGFP/MHV-68 (MOI = 2) at 5, 8, 12, or 24 h postinfection and used to generate labeled cDNA probes as described in Materials and Methods for hybridization to the MHV-68 viral DNA arrays. The signal from each viral DNA spot was normalized against the cellular GAPDH (glyceraldehyde-3-phosphate dehydrogenase) signal on the same membrane. The fold of induction was calculated by dividing the normalized values of the AC-RTA arrays with those of the EGFP arrays. These values and their corresponding MHV-68 ORFs at different times postinfection are shown by bar graphs, and the bars are ordered based on the descending total fold of increase. The paired *t* test was used to analyze statistical significance of the differences (black bars, $P < 0.01$, light blue bars, $P < 0.05$, light yellow bars, $P > 0.05$).

similar to those formed by the C-RTA virus (48), indicating that the AC-RTA virus replicated or spread faster than WT. Next, we compared the replication ability of the AC-RTA virus in BHK-21 cells with WT and C-RTA viruses by performing growth curve analysis. In the single-step growth study, the three viruses replicated almost indistinguishably from each other (Fig. 2D). However, in the multiple-step growth experiment, AC-RTA replicated and produced higher titers than did the WT virus at 48, 72, and 96 h postinfection (Fig. 2E). The C-RTA virus also replicated to a higher level than the WT (Fig. 2E), which was consistent with our previous report (48). The results indicate that the modifications introduced in the AC-RTA virus do not reduce, but rather enhance, viral replication *in vitro*.

We then conducted a genome-wide analysis of viral gene expression using arrays generated in the laboratory with DNA fragments derived from individual MHV-68 ORFs (42). The viral gene expression profile of C-RTA was previously carried out in comparison to a recombinant virus that has an enhanced green fluorescence protein (EGFP) expression cassette inserted at the left end of the genome (EGFP/MHV-68) (42). Here, we performed a similar comparative analysis with RNA harvested at different times after infection. As shown in Fig. 3, the most significant difference was observed at 5 h postinfection at which time the majority of the 85 viral genes were enhanced with folds of increase ranging from 2 to 7, and the most highly activated viral genes (>6-fold) were the ORFs encoding the structural proteins (ORF67, -64, and -68). As expected, at all time points examined, RTA was highly expressed from the AC-RTA virus, which contains an ectopic RTA expression cassette driven by a strong promoter. Consistent with the role of RTA in activating transcription, overexpression of RTA increased viral gene expression during infection of the AC-RTA virus, a phenotype similar to that of the C-RTA virus (42). The increase in the viral gene expression became moderate and less significant at later times postinfection.

Acute infection of AC-RTA in the lung is attenuated. Intranasal inoculation of MHV-68 into mice produces an acute productive infection in the lung, which is cleared by the im-

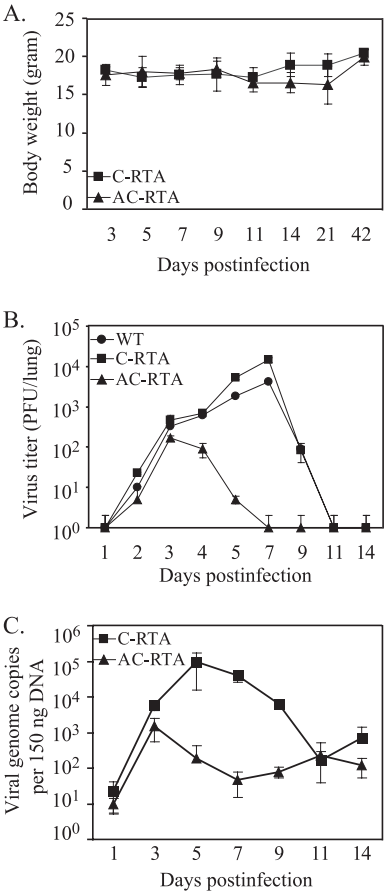

FIG. 4. Replication of AC-RTA virus in the lung. (A) Body weights of BALB/c mice infected with 500 PFU of C-RTA or AC-RTA. The data were compiled from three mice infected with C-RTA (■) and five mice infected with AC-RTA (▲). (B) Virus titers in the lungs. The lungs were removed from infected mice at the indicated times postinfection, and the tissue homogenates were used for plaque assays to determine the virus titers. (C) Quantitation of the viral DNA in the lungs. The copy numbers of viral genomes in the tissue homogenates were measured by TaqMan quantitative PCR using a probe and primers to ORF65.

mune system within 2 weeks after infection. Generally, we did not observe any sickness in BALB/c mice infected with 500 PFU of the WT. In mice examined over times after infection with AC-RTA or C-RTA, there was no detectable loss in their body weights (Fig. 4A). Next, the virus titers in the lung at various times postinfection were determined by plaque assays. The AC-RTA virus replicated similarly and generated comparable titers to WT and the C-RTA virus for the first 3 days after infection (Fig. 4B). However, the virus titers of AC-RTA declined after day 3 postinfection, whereas replication of the other two viruses continued until day 7, resulting in a nearly 100-fold difference in the peak titers between AC-RTA (day 3) and WT or C-RTA infection (day 7). The results clearly indicated an attenuation of AC-RTA in the acute lung infection. A higher inoculation dose of 10^5 PFU did not overcome the attenuation of AC-RTA in the lung (data not shown).

We also examined the copy number of viral genomes by real-time PCR. Consistent with the results of virus titers, the levels of viral genomes in the mice infected with AC-RTA reached the peak at day 3 and then decreased afterward, while those in the mice infected with C-RTA continued to increase until day 5 postinfection (Fig. 4C). Consequently, there was almost 100-fold less viral DNA in the lungs of mice infected with AC-RTA compared to that in the lungs of mice infected with C-RTA, which shows that acute infection of AC-RTA in the lung is attenuated.

AC-RTA virus fails to establish latency in the spleen. After being cleared from the lung by the host immunity, MHV-68 establishes latency in the spleen with a peak viral load at day 14 (20, 58, 60). At this peak time of viral latency, the mice exhibit a mononucleosislike symptom due to an amplification of lymphocytes, which causes a significant increase in the spleen weight (splenomegaly) (64). We thus examined the spleen sizes of infected mice over time. For WT and C-RTA, viral infection led to a gradual increase in the spleen weights, starting from day 11 and reaching the peak at day 14 (Fig. 5A). Nevertheless, the spleens of mice infected with C-RTA were significantly smaller than those infected with the WT. In contrast, we saw no increase in the spleen sizes of mice infected with AC-RTA, indicating that AC-RTA does not induce mononucleosis-like splenomegaly. To determine the viral latent load in the spleen, single cell suspensions were obtained from the spleens harvested at days 14, 21, and 42 postinfection. We first quantified the levels of viral genomes in the splenocytes by real-time PCR using primers specifically to amplify a region in ORF65 (48). Overall, >10-fold fewer viral genomes were detected in the splenocytes from the mice infected with C-RTA than those from mice infected with the WT (Fig. 5B). Importantly, in cells from mice infected with AC-RTA, the levels of viral genomes were below the detection limit at all time points examined.

To further examine viral latency in the spleen, the splenocytes were used for bothinfectious-center (Fig. 5C and E) and ex vivo limiting-dilution (Fig. 5D and F) assays (60, 70). None of the five mice infected with AC-RTA had any detectable viral reactivation in the spleen at either the peak time, day 14 postinfection (Fig. 5C and D), or a later time, day 21 postinfection (Fig. 5E and F). In agreement with the previous study that latency of the C-RTA virus was attenuated in the spleen, ~100-fold less viral reactivation was detected at day 14 postinfection in the splenocytes from mice infected with C-RTA compared to those from the mice infected with the WT. At day 42 postinfection, ~10 infectious centers per 10^7 splenocytes could be detected in the mice infected with WT, but no infectious centers were detected in the mice infected with either the C-RTA or AC-RTA virus (data not shown). Taken together, while infection of C-RTA still leads to a low level of latency in the spleen, infection of AC-RTA results in no detectable latency.

AC-RTA virus replication is concentrated in the inoculation site. To systemically monitor virus replication *in vivo*, we used a noninvasive bioluminescence imaging approach. This is achieved by introducing an expression cassette of firefly luciferase driven by a viral M3 promoter into the MHV-68 genome and imaging the luciferase activity in mice with a cooled CCD camera after injection of luciferin (29). The firefly luciferase expression cassette (M3-FL) was engineered into the genomes of WT and AC-RTA using a BAC mutagenesis system. The resultant viruses, M3-FL/MHV-68 and M3-FL/AC-RTA, were individually used to infect mice. At the indicated times postin-

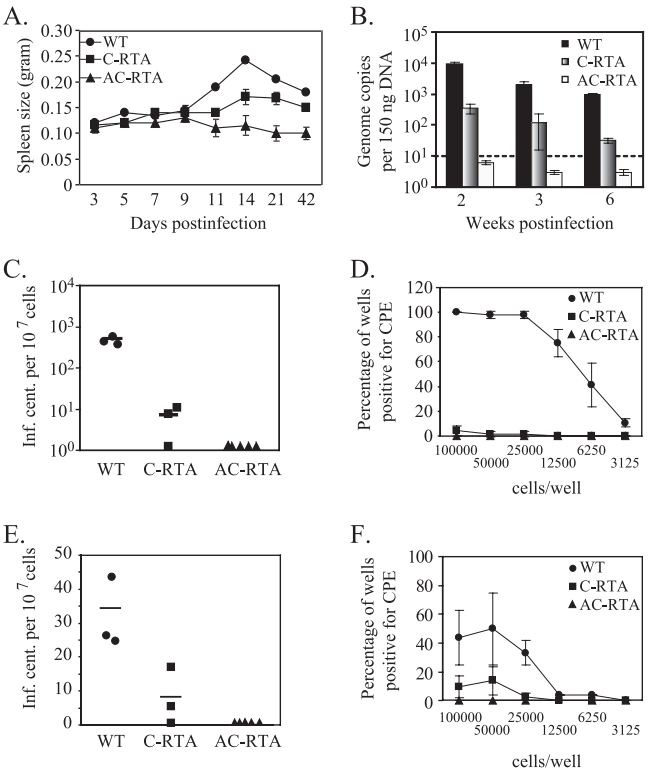

FIG. 5. Latent infection of AC-RTA in the spleen. (A) The spleen weights of mice infected with 500 PFU of WT, AC-RTA, or C-RTA. (B) Quantitation of the viral DNA in the splenocytes from WT-, C-RTA-, or AC-RTA-infected mice. Total DNA was isolated from splenocytes, and 150 ng of genomic DNA was used for TaqMan quantitative PCR assays. The dotted line represents the limit of confident measurement per 150 ng of DNA. (C to F) Levels of reactivating viruses in the spleens of mice infected with WT, AC-RTA or C-RTA. The single cell suspensions were obtained from the spleens harvested at day 14 (C and D) and at day 21 (E and F) postinfection. The reactivating viruses were measured by infectious center assays (C and E) and ex vivo limiting dilution assays (D and F). In panels C and E, the numbers of infectious centers from individual mice are shown, and the solid lines represent the averages of infectious centers in each group of mice. In panels D and F, the symbols represent the averages and the standard deviations are shown as error bars. The data in each panel were compiled from three mice infected with WT or C-RTA and from five mice infected with AC-RTA.

fection, three mice in each group were examined for the luciferase expression with a CCD camera and the representative images are shown in Fig. 6. The luminescence signals in the mice infected with M3-FL/MHV-68 (the left mouse in the images) were first detected in the nasal/oral areas and lungs as early as day 3, peaked at day 7, and then cleared off from these sites by day 14 postinfection. There were no signals in the spleen until day 14, the peak time of viral latency, after which the signals gradually reduced and became minimally detectable by day 21 postinfection. The kinetics of the luminescence signals in the lung and spleen were consistent with the virus replication kinetics obtained with virological methods (Fig. 4B). Thus, the bioluminescence *in vivo* imaging provides a valid approach to monitor the progression of viral infection in live mice.

Using this noninvasive method, we found a different pattern of bioluminescence in the mice infected with M3-FL/AC-RTA compared to those infected with M3-FL/MHV-68. The signals in mice infected with M3-FL/AC-RTA were largely limited in the nasal/oral area where the virus was inoculated and remained detectable for over 14 days after infection. It was also noted that the signals were reduced between day 7 and day 11 postinfection but then increased again between day 11 and day 14 postinfection. This increase was observed for all of three mice infected with M3-FL/AC-RTA (data not shown). We then examined the presence of the virus by PCR and found that the viral genomes were detected in the brain tissues of mice infected with M3-FL/AC-RTA, as well as in those of mice infected with M3-FL/MHV-68 (data not shown). This is not surprising since it was previously reported that MHV-68 can gain access to the central nervous system after intranasal inoculation (62). The viral DNA was at a lower level in the brain tissues of mice infected with M3-FL/MHV-68, which is probably the reason for that bioluminescence imaging was unable to detect any luciferase activity. Nevertheless, the signals in the head area of mice infected with M3-FL/AC-RTA were subsided after 3 weeks postinfection. In addition to the head area, there were limited luminescence signals detected in the lung at day 3 postinfection. No luminescence signals were detected in the spleen area. These observations agrees with the virological result in which the titers of AC-RTA in the lung peaked at day 3 postinfection and declined thereafter (Fig. 4B) and are also consistent with the latency result that no detectable viral DNA was found in the spleen at weeks 2, 3, and 6 postinfection of AC-RTA (Fig. 5B). The bioluminescence work further supports the conclusion that the AC-RTA virus is not only attenuated in the acute lung infection but also greatly compromised in its ability to establish latency in the spleen.

AC-RTA virus protects mice against WT MHV-68 challenge. Previously, we showed that C-RTA afforded protection against challenge infections of WT MHV-68 (48). With an additional deletion of several latency-associated genes, AC-RTA displayed attenuated replication in the lung and undetectable establishment of latency in the spleen; such results raised a question whether AC-RTA was capable of eliciting protective immunity from subsequent challenge infections. To answer this question, we vaccinated mice with 500 PFU of AC-RTA and then 90 days later challenged them intranasally with 500 PFU of the WT. We assayed the virus titers in the lung harvested at day 7 postchallenge (the peak time of acute infection). As shown in Fig. 7A, the mice vaccinated with either C-RTA or AC-RTA had virus titers below the detection limit after challenge infections, indicating that vaccination of AC-RTA was equally effective as vaccination of C-RTA in providing protection. We then examined the establishment of latency at day 14 after challenge (the peak of latency in the spleen) and did not detect any reactivating virus in the AC-RTA-vaccinated mice using an infectious center assay or ex vivo limiting dilution assay (Fig. 7B and C). In comparison, the mock-vaccinated mice had an average of 973 infectious centers per 10^7 splenocytes after challenges of WT; a low but detectable level of reactivating virus could be found in the WT-challenged mice that were previously vaccinated with C-RTA (Fig. 7B and C). We also measured the copy number of viral genomes in the splenocytes by real-time PCR. The levels of viral DNA were below the detection limit in the samples from WT-challenged

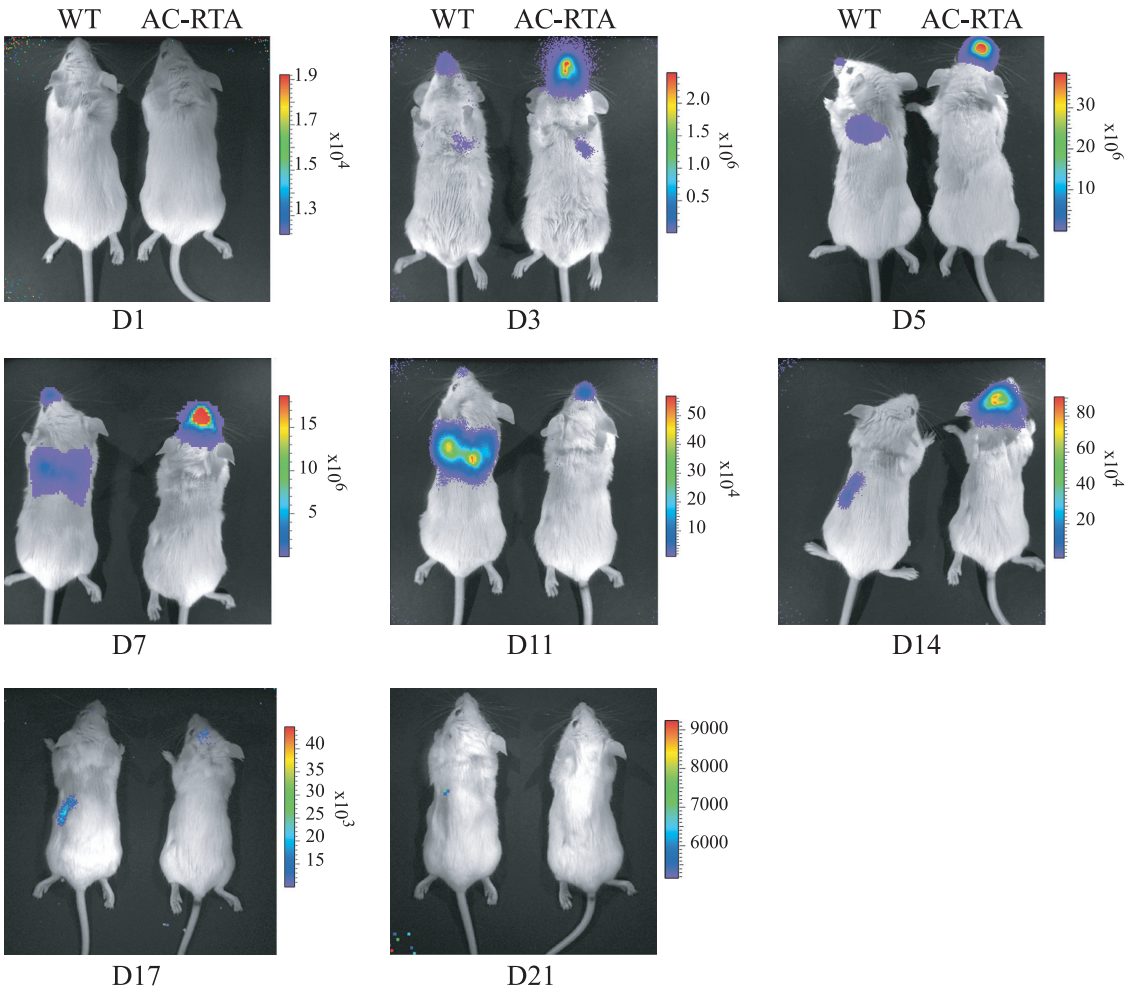

FIG. 6. Bioluminescence imaging of firefly luciferase in mice infected with M3-FL/MHV-68 or M3-FL/AC-RTA viruses. Mice were infected with 5×10^5 PFU of M3-FL/MHV-68 or M3-FL/AC-RTA. On each panel, the mouse shown on the left was infected with M3-FL/MHV-68 and the one shown on the right was infected with M3-FL/AC-RTA.The bioluminescence imaging of luciferase expression was performed on the same mice at different days postinfection (as labeled under each panel). Representative images obtained from a 5- to 30-min acquisition are shown. The pseudocolor scale shows the relative photon flux on each image. Note that the minimum and maximum values for photon flux differ among the images.

mice that were previously vaccinated with AC-RTA, while an average as high as 4,402 copies of viral genomes per 150 ng of genomic DNA was found in the mock-vaccinated mice (Fig. 7D). Prior vaccination with C-RTA reduced the burden of viral genomes by 10-fold (346 copies/150 ng of genomic DNA) (Fig. 7D).

Next, we sought to determine whether intranasal vaccination was able to protect mice from the subsequent challenge via an intraperitoneal route. The mice were first mock infected or infected intranasally with either WT or AC-RTA, and 4 months later they were challenged intraperitoneally with the WT virus. The latent viral loads in the spleens of mice at 14 days postchallenge were assessed by infectious center assays. In contrast to the mock-vaccinated mice where thousands of infectious centers per 10^7 cells were detected, there were no detectable reactivating viruses in mice vaccinated with WT or in those vaccinated with AC-RTA (Fig. 7E). These results clearly demonstrated that AC-RTA can prevent the establishment of latency by the challenged WT virus and thus provides a better vaccine virus candidate than C-RTA. Since AC-RTA does not have ORF72, M11 or ORF73, our data suggest that these three genes are not required to elicit an immunity that can protect mice from latency establishment of MHV-68.

Both cellular and humoral immune responses are elicited by infection of AC-RTA. Since AC-RTA was capable of inducing protective immunity in mice against subsequent challenge, we examined humoral and cellular immunity elicited by the AC-RTA virus. Virus-specific IgG was detected by ELISA in the sera collected from mice infected with AC-RTA at 6 weeks postinfection (Fig. 8A). Although the antibody titers appeared lower compared to the titers in the sera from WT-infected mice, the difference does not reach statistical significance ($P = 0.07$, Student t test). To measure virus-specific T-cell responses, we used tetramer staining of a well-characterized lytic epitope identified in C57BL/6 mice derived from ORF6 (p56) (54). At day 21 postinfection, both AC-RTA and WT elicited CD8-responses to ORF6 in the spleen (Fig. 8B and C). Therefore, our data indicate that infection of AC-RTA elicits both T-cell and antibody responses against lytic antigens.

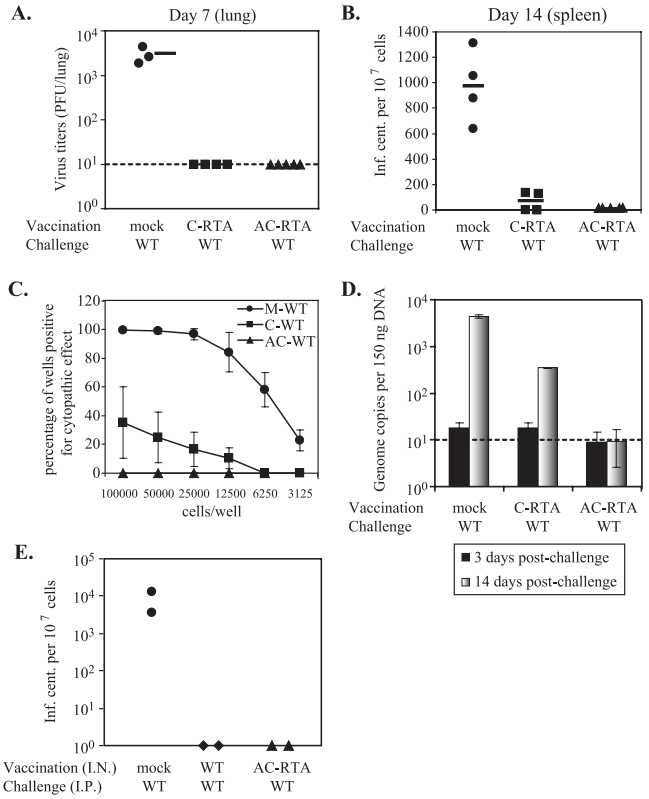

FIG. 7. WT virus challenge in mice vaccinated with AC-RTA virus. For panels A to D, BALB/c mice were mock vaccinated or vaccinated intranasally with 500 PFU of C-RTA or AC-RTA. At 3 months postvaccination, mice were challenged intransally with 500 PFU of the WT virus. (A) Virus titers in the lungs at 7 days postchallenge. The lung homogenates were obtained, and the titers were determined by using plaque assays. The titers of individual mice are shown, and the average of each group is indicated by an adjacent solid line. The detection limit of plaque assays is shown by a dotted line. (B and C) The levels of reactivating viruses at 14 days postchallenge. Single cell suspensions of splenocytes were prepared; the reactivating viruses were quantitated by infectious center assays (B) and ex vivo limiting dilution assays (C). In panel B, the number of infectious centers of each individual mouse is shown and the average of each group is represented by an adjacent solid line. In panel C, the symbols represent the averages, and the standard deviations are indicated as error bars. (D) Quantitation of viral DNA in the spleens harvested at 3 and 14 days postchallenge. Total DNA was isolated from splenocytes and used for TaqMan quantitative PCR assays. The dotted line represents the limit of confident measurement per 150 ng of DNA. The data were compiled from four WT-challenged mice that were mock or C-RTA vaccinated and five mice that were AC-RTA vaccinated. For panel E, BALB/c mice were mock vaccinated or vaccinated intranasally with 10^4 PFU of WT or AC-RTA and, at 4 months postvaccination, the mice were challenged intraperitoneally with 500 PFU of the WT virus. (E) The levels of reactivating viruses in the spleen of mice at day 14 after intraperitoneal challenge were quantitated by infectious center assays.

Because AC-RTA does not establish any detectable latency, we next examined whether the cellular responses to latent antigens following infection were affected. A tetramer of a previously identified latent epitope in BALB/c mice derived from M2 was used for this study (28). Although infection of WT generated M2-specific CD8 responses in the spleen as well as in the lung at day 20 postinfection, there was very little M2-specific response elicited by infection of AC-RTA (Fig. 8D and E). Similar results were obtained by using intracellular IFN-γ staining (Fig. 8F and G), suggesting that AC-RTA does not induce significant cellular immunity to latent antigens.

DISCUSSION

We and others have previously shown that overexpression of RTA significantly decreases, but not completely eliminates, latency of the virus in the spleen (7, 48). However, a further reduced capacity of establishing latency is essential for the development of a live attenuated virus as a vaccine for gammherpesviruses. Therefore, we constructed a recombinant virus that has an RTA expression cassette driven by a highly active promoter inserted into the genome with a simultaneous deletion of ORF72, M11, or ORF73, which are essential for viral latency and reactivation (13, 23, 25, 27, 45, 67). In this report, we showed that this recombinant virus, AC-RTA, is replication-competent *in vitro* but attenuated in the acute infection of the lung and has no detectable latency establishment in the spleen. As a result, AC-RTA serves as an ideal strategy for vaccination against gammaherpesviruses. Next, we demonstrated that immunization of AC-RTA is able to reduce latency from a subsequent WT challenge infection to a level below the detection limit. In addition, we have shown that AC-RTA is able to efficiently induce virus-specific IgG and CD8 T-cell responses to a lytic epitope. Our findings suggest that with an efficient approach for genetic engineering of herpesviruses, it may be possible to apply a similar strategy to construct a live-attenuated human herpesvirus devoid of latency that can provide sufficient immunity to prevent infection.

Upregulation of RTA enhances viral gene expression and *in vitro* lytic replication in fibroblasts. However, after intranasal infection of mice, viral replication of AC-RTA in the lung was compromised compared to that of WT in that the virus titers in the AC-RTA-infected mice decreased after 3 days, whereas in the WT-infected mice the titers continued to increased until 7 days after infection (Fig. 4B). This earlier decline of AC-RTA infection in the lung may result from a deficit associated with *in vivo* replication of the virus or a more vigorous immune response induced by the virus. Our previous C-RTA virus, with intact latency-associated genes, replicated comparably to WT in the lung until day 7 but was cleared faster afterward (48). Another recombinant virus with RTA overexpression had a similar phenotype of faster clearance (43). One clue about the mechanism underlying the earlier decline of AC-RTA infection in the lung comes from the bioluminescence imaging result; compared to WT infection, AC-RTA infection produced much stronger signals in the nasal/oral area where the virus was inoculated (Fig. 6). Since the expression of luciferase is under the control of a RTA-responsive viral M3 promoter, the enhancement clearly indicates that overexpression of RTA upregulates luciferase expression and most likely MHV-68 viral genes as well. This upregulation of viral gene expression may in turn initiate an earlier and stronger antiviral immune response that limits infection of AC-RTA. Alternatively, simultaneous deletion of ORF72, M11, and ORF73 may affect acute viral infection in the lungs. It has been shown that the lack of ORF72 or M11 causes no effects on viral acute infection in the lungs. However, recent studies have implicated that ORF73 may be required for efficient viral lytic replication (21, 45). To

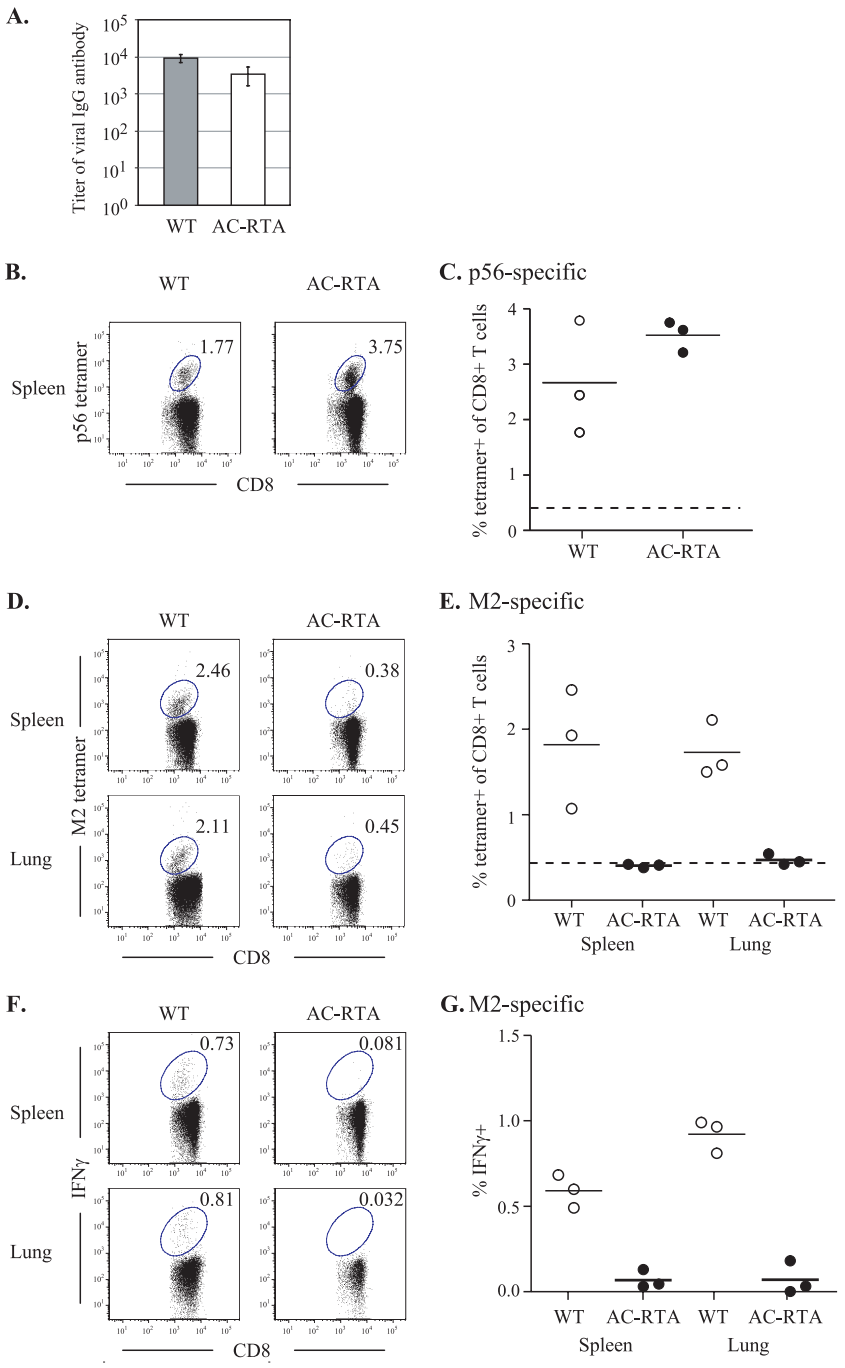

FIG. 8. Humoral and cellular responses in the infected mice. (A) Virus-specific IgG titers. BALB/c mice were intranasally infected with 500 PFU of WT or AC-RTA and at 6-week postinfection, the sera were collected for ELISA. The averages and standard deviations were generated from three mice for each group. (B and C) CD8 T-cell responses to $ORF6_{487-495}$ (p56). C57BL/6 mice were intranasally infected with 400 PFU of WT or AC-RTA virus and, 21 days later, $CD8^+$ T cells were harvested and stained with $D^b/ORF6_{487-495}$ tetramer. Representative dot plots are shown are in panel B, and the percentages of $CD8^+$ T cells bound with ORF6 (p56) tetramer for individual mice are shown in panel C. The dotted line is the level of tetramer staining of uninfected mice. (D to G) The CD8-T cell responses to $M2_{91-99}$. BALB/c mice were intranasally infected with 400 PFU of WT or AC-RTA virus and, 20 days later, $CD8^+$ T cells were harvested from spleen or lungs and stained with $K^d/M2_{91-99}$ tetramer (D and E). Panel D shows representative dot plots, and the percentages of M2-bound $CD8^+$ T cells from individual mice are shown in panel E. The dotted line is the level of tetramer staining of uninfected mice. Statistical significance of the differences were analyzed by using the Student *t* test (spleen, $P = 0.0250$; lung, $P = 0.0029$). The M2-specific responses were also analyzed by intracellular cytokine staining (F and G). $CD8^+$ T cells were stimulated for 5 h ex vivo with $M2_{91-99}$ peptide-pulsed congenic (Thy1.1) splenocytes in the presence of brefeldin A and then permeabilized and stained for intracellular accumulation of IFN-γ. Panel F shows representative dot plots, and the percentages of $CD8^+$ T cells that are IFN-γ^+ minus the unstimulated background controls from individual mice are shown in panel G. Statistical significance of the differences were analyzed by using the Student *t* test (spleen, $P = 0.0012$; lung, $P = 0.0004$).

distinguish these possibilities and determine whether the attenuation of AC-RTA is mediated by the immune response, we will need to perform an infection kinetic study in immunocompromised mice.

Lack of latency is a prerequisite for using a live virus as a vaccine for gammaherpesviruses. Nevertheless, it is generally thought that persistent infection can constantly restimulate the immune system. Thus, it is a concern whether a latency-deficient virus can generate a long-term immunity to provide protection against WT infection. However, it has been shown that chronic exposure to antigens can cause functional impairment in antigen-specific CD8-T cells (71) and have negative effects on the development of memory T cells (72). In the present study, we showed that a single vaccination with the AC-RTA virus provides protection against the WT MHV-68 challenge 3 months after vaccination. The data suggest that the immune protection stimulated by a transient acute infection can be long-lived.

The result that AC-RTA is able to inhibit latency establishment from a subsequent challenge infections suggests that immunity targeted to ORF72, M11, and ORF73 is not required for protection and not even required for preventing the establishment of latency. This is somewhat surprising, since only a few viral genes are expressed during latency, including ORF72, M11, and ORF73. Nevertheless, it is well known that one important strategy for herpesviruses to persist for a lifetime in the host is the utilization of multiple immune evasion mechanisms. Therefore, even though some viral genes are expressed in latently infected cells, they may not be detectable for the immune system, as has been proven the case for ORF73 (4). Although another latency-associated antigen, M2, is not deleted from AC-RTA, the T-cell analysis showed that very little M2-specific CD8 response was elicited by AC-RTA compared to WT (Fig. 8D to G). Since AC-RTA is able to afford protection against challenge infection of the wild-type MHV-68, the immunity targeted to M2 perhaps does not play a role in the protective effects of AC-RTA.

Herpesviruses, with an enormous coding capacity, encode several genes to evade or modulate the immune responses for their survival in the host. For optimal use as a vaccine, eliminating viral genes that are responsible for inhibiting the host responses may improve their immunogenicity. One example for MHV-68 is the K3 protein, a homologue of KSHV K3, which downregulates the expression of major histocompatibility complex I on the infected cell surface by a ubiquitin ligase function (8). *In vivo* studies have found that the frequency of virus-specific $CD8^+$ cytotoxic T cells was increased in mice infected with the K3-deficient MHV-68 (56). Thus, removal of K3 may enhance T-cell responses induced by a vaccine virus. Previously, we and others have conducted systemic mutagenesis on the MHV-68 genome with the goal of enhancing our understanding of the virus-host interactions. The knowledge of the function of individual genes and an efficient genetic mutagenesis system of MHV-68 will allow us to have a rational design of a live attenuated virus as a vaccine and test candidates in mouse infection models. Although MHV-68 infection of mice may not recapitulate all aspects of KSHV or EBV infection of humans, MHV-68 has provided us with an important experimental model for testing some proof of principles in vaccine strategies for gammaherpesviruses. Furthermore, considering that MHV-68, EBV, and KSHV share at least 80% sequence homology, and many proteins required for lytic replication and functions required for latency are conserved, the results obtained from MHV-68 can have significant implications to human gammaherpesviruses. As we have shown here, a strategy of overexpressing a viral immediate-early transcriptional activator (RTA) and deleting latent genes can be used with human gammaherpesviruses to generate a latency-deficient virus as a safe vaccine approach. It remains unclear whether sterilizing immunity to prevent herpesvirus infection in humans can be achieved by vaccination. However, one should recognize that a vaccine that can reduce the viral latent load would be still valuable to minimize the burden of virus-associated diseases.

ACKNOWLEDGMENTS

This study was supported by National Institutes of Health grants DE18337 (T.-T.W.), AI42927 (M.A.B.), CA91791, DE14153, and DE15752 and by the Stop Cancer Foundation (R.S.).

We thank Timothy Lu for editing of the manuscript and assistance with the ELISA and Yuri Shindo and Victoria Bender for editing of the manuscript.

REFERENCES

1. **Arico, E., K. A. Robertson, F. Belardelli, M. Ferrantini, and A. A. Nash.** 2004. Vaccination with inactivated murine gammaherpesvirus 68 strongly limits viral replication and latency and protects type I IFN receptor knockout mice from a lethal infection. Vaccine **22:**1433–1440.
2. **Ballestas, M. E., P. A. Chatis, and K. M. Kaye.** 1999. Efficient persistence of extrachromosomal KSHV DNA mediated by latency-associated nuclear antigen. Science **284:**641–644.
3. **Becker, S. D., M. Bennett, J. P. Stewart, and J. L. Hurst.** 2007. Serological survey of virus infection among wild house mice (*Mus domesticus*) in the UK. Lab. Anim. **41:**229–238.
4. **Bennett, N. J., J. S. May, and P. G. Stevenson.** 2005. Gamma-herpesvirus latency requires T-cell evasion during episome maintenance. PLoS Biol. **3:**e120.
5. **Blasdell, K., C. McCracken, A. Morris, A. A. Nash, M. Begon, M. Bennett, and J. P. Stewart.** 2003. The wood mouse is a natural host for murid herpesvirus 4. J. Gen. Virol. **84:**111–113.
6. **Blaskovic, D., M. Stancekova, J. Svobodova, and J. Mistrikova.** 1980. Isolation of five strains of herpesviruses from two species of free living small rodents. Acta Virol. **24:**468.
7. **Boname, J. M., H. M. Coleman, J. S. May, and P. G. Stevenson.** 2004. Protection against wild-type murine gammaherpesvirus-68 latency by a latency-deficient mutant. J. Gen. Virol. **85:**131–135.
8. **Boname, J. M., and P. G. Stevenson.** 2001. MHC class I ubiquitination by a viral PHD/LAP finger protein. Immunity **15:**627–636.
9. **Brambilla, L., V. Boneschi, E. Berti, M. Corbellino, and C. Parravicini.** 1996. HHV8 cell-associated viraemia and clinical presentation of Mediterranean Kaposi's sarcoma. Lancet **347:**1338.
10. **Bridgeman, A., P. G. Stevenson, J. P. Simas, and S. Efstathiou.** 2001. A secreted chemokine binding protein encoded by murine gammaherpesvirus-68 is necessary for the establishment of a normal latent load. J. Exp. Med. **194:**301–312.
11. **Cesarman, E., Y. Chang, P. S. Moore, J. W. Said, and D. M. Knowles.** 1995. Kaposi's sarcoma-associated herpesvirus-like DNA sequences in AIDS-related body-cavity-based lymphomas. N. Engl. J. Med. **332:**1186–1191.
12. **Chang, Y., E. Cesarman, M. S. Pessin, F. Lee, J. Culpepper, D. M. Knowles, and P. S. Moore.** 1994. Identification of herpesvirus-like DNA sequences in AIDS-associated Kaposi's sarcoma. Science **266:**1865–1869.
13. **de Lima, B. D., J. S. May, S. Marques, J. P. Simas, and P. G. Stevenson.** 2005. Murine gammaherpesvirus 68 bcl-2 homologue contributes to latency establishment in vivo. J. Gen. Virol. **86:**31–40.
14. **Dittmer, D., M. Lagunoff, R. Renne, K. Staskus, A. Haase, and D. Ganem.** 1998. A cluster of latently expressed genes in Kaposi's sarcoma-associated herpesvirus. J. Virol. **72:**8309–8315.
15. **Dupin, N., C. Fisher, P. Kellam, S. Ariad, M. Tulliez, N. Franck, E. van Marck, D. Salmon, I. Gorin, J. P. Escande, R. A. Weiss, K. Alitalo, and C. Boshoff.** 1999. Distribution of human herpesvirus-8 latently infected cells in Kaposi's sarcoma, multicentric Castleman's disease, and primary effusion lymphoma. Proc. Natl. Acad. Sci. U. S. A. **96:**4546–4551.
16. **Efstathiou, S., Y. M. Ho, S. Hall, C. J. Styles, S. D. Scott, and U. A. Gompels.** 1990. Murine herpesvirus 68 is genetically related to the gammaherpesvi-

ruses Epstein-Barr virus and herpesvirus saimiri. J. Gen. Virol. **71:**1365–1372.
17. **Efstathiou, S., Y. M. Ho, and A. C. Minson.** 1990. Cloning and molecular characterization of the murine herpesvirus 68 genome. J. Gen. Virol. **71:** 1355–1364.
18. **Fickenscher, H., B. Biesinger, A. Knappe, S. Wittmann, and B. Fleckenstein.** 1996. Regulation of the herpesvirus saimiri oncogene *stpC*, similar to that of T-cell activation genes, in growth-transformed human T lymphocytes. J. Virol. **70:**6012–6019.
19. **Fickenscher, H., C. Bokel, A. Knappe, B. Biesinger, E. Meinl, B. Fleischer, B. Fleckenstein, and B. M. Broker.** 1997. Functional phenotype of transformed human αβ and γδ T cells determined by different subgroup C strains of herpesvirus Saimiri. J. Virol. **71:**2252–2263.
20. **Flano, E., S. M. Husain, J. T. Sample, D. L. Woodland, and M. A. Blackman.** 2000. Latent murine gamma-herpesvirus infection is established in activated B cells, dendritic cells, and macrophages. J. Immunol. **165:**1074–1081.
21. **Forrest, J. C., C. R. Paden, R. D. Allen III, J. Collins, and S. H. Speck.** 2007. ORF73-null murine gammaherpesvirus 68 reveals roles for mLANA and p53 in virus replication. J. Virol. **81:**11957–11971.
22. **Fowler, P., and S. Efstathiou.** 2004. Vaccine potential of a murine gammaherpesvirus-68 mutant deficient for ORF73. J. Gen. Virol. **85:**609–613.
23. **Fowler, P., S. Marques, J. P. Simas, and S. Efstathiou.** 2003. ORF73 of murine herpesvirus-68 is critical for the establishment and maintenance of latency. J. Gen. Virol. **84:**3405–3416.
24. **Friborg, J., Jr., W. P. Kong, C. C. Flowers, S. L. Flowers, Y. Sun, K. E. Foreman, B. J. Nickoloff, and G. J. Nabel.** 1998. Distinct biology of Kaposi's sarcoma-associated herpesvirus from primary lesions and body cavity lymphomas. J. Virol. **72:**10073–10082.
25. **Gangappa, S., L. F. van Dyk, T. J. Jewett, S. H. Speck, and H. W. T. Virgin.** 2002. Identification of the in vivo role of a viral bcl-2. J. Exp. Med. **195:**931–940.
26. **Hall, K. T., M. S. Giles, D. J. Goodwin, M. A. Calderwood, I. M. Carr, A. J. Stevenson, A. F. Markham, and A. Whitehouse.** 2000. Analysis of gene expression in a human cell line stably transduced with herpesvirus saimiri. J. Virol. **74:**7331–7337.
27. **Hoge, A. T., S. B. Hendrickson, and W. H. Burns.** 2000. Murine gammaherpesvirus 68 cyclin D homologue is required for efficient reactivation from latency. J. Virol. **74:**7016–7023.
28. **Husain, S. M., E. J. Usherwood, H. Dyson, C. Coleclough, M. A. Coppola, D. L. Woodland, M. A. Blackman, J. P. Stewart, and J. T. Sample.** 1999. Murine gammaherpesvirus M2 gene is latency-associated and its protein a target for $CD8^+$ T lymphocytes. Proc. Natl. Acad. Sci. U. S. A. **96:**7508–7513.
29. **Hwang, S., T. T. Wu, L. M. Tong, K. S. Kim, D. Martinez-Guzman, A. D. Colantonio, C. H. Uittenbogaart, and R. Sun.** 2008. Persistent gammaherpesvirus replication and dynamic interaction with the host in vivo. J. Virol. **82:**12498–12509.
30. **Jacoby, M. A., H. W. T. Virgin, and S. H. Speck.** 2002. Disruption of the M2 gene of murine gammaherpesvirus 68 alters splenic latency following intranasal, but not intraperitoneal, inoculation. J. Virol. **76:**1790–1801.
31. **Jia, Q., T. T. Wu, H. I. Liao, V. Chernishof, and R. Sun.** 2004. Murine gammaherpesvirus 68 open reading frame 31 is required for viral replication. J. Virol. **78:**6610–6620.
32. **Kieff, E., and A. B. Rickinson.** 2001. Epstein-Barr virus and its replication, p. 2511–2627. *In* D. M. Knipe and P. M. Howley (ed.), Fields virology, vol. 2. Lippincott/The Williams & Wilkins Co., Philadelphia, PA.
33. **Ku, B., J. S. Woo, C. Liang, K. H. Lee, H. S. Hong, X. E, K. S. Kim, J. U. Jung, and B. H. Oh.** 2008. Structural and biochemical bases for the inhibition of autophagy and apoptosis by viral BCL-2 of murine gamma-herpesvirus 68. PLoS Pathog. **4:**e25.
34. **Lan, K., D. A. Kuppers, S. C. Verma, and E. S. Robertson.** 2004. Kaposi's sarcoma-associated herpesvirus-encoded latency-associated nuclear antigen inhibits lytic replication by targeting Rta: a potential mechanism for virus-mediated control of latency. J. Virol. **78:**6585–6594.
35. **Levy, R., and R. A. Miller.** 1990. Therapy of lymphoma directed at idiotypes. J. Natl. Cancer Inst. Monogr. **1990:**61–68.
36. **Li, Q., F. Zhou, F. Ye, and S. J. Gao.** 2008. Genetic disruption of KSHV major latent nuclear antigen LANA enhances viral lytic transcriptional program. Virology **379:**234–244.
37. **Liu, L., E. J. Usherwood, M. A. Blackman, and D. L. Woodland.** 1999. T-cell vaccination alters the course of murine herpesvirus 68 infection and the establishment of viral latency in mice. J. Virol. **73:**9849–9857.
38. **Liu, S., I. V. Pavlova, H. W. T. Virgin, and S. H. Speck.** 2000. Characterization of gammaherpesvirus 68 gene 50 transcription. J. Virol. **74:**2029–2037.
39. **Lukac, D. M., R. Renne, J. R. Kirshner, and D. Ganem.** 1998. Reactivation of Kaposi's sarcoma-associated herpesvirus infection from latency by expression of the ORF 50 transactivator, a homolog of the EBV R protein. Virology **252:**304–312.
40. **Mackett, M., J. P. Stewart, V. P. S. de, M. Chee, S. Efstathiou, A. A. Nash, and J. R. Arrand.** 1997. Genetic content and preliminary transcriptional analysis of a representative region of murine gammaherpesvirus 68. J. Gen. Virol. **78:**1425–1433.
41. **Marques, S., S. Efstathiou, K. G. Smith, M. Haury, and J. P. Simas.** 2003. Selective gene expression of latent murine gammaherpesvirus 68 in B lymphocytes. J. Virol. **77:**7308–7318.
42. **Martinez-Guzman, D., T. Rickabaugh, T. T. Wu, H. Brown, S. Cole, M. J. Song, L. Tong, and R. Sun.** 2003. Transcription program of murine gammaherpesvirus 68. J. Virol. **77:**10488–10503.
43. **May, J. S., H. M. Coleman, B. Smillie, S. Efstathiou, and P. G. Stevenson.** 2004. Forced lytic replication impairs host colonization by a latency-deficient mutant of murine gammaherpesvirus-68. J. Gen. Virol. **85:**137–146.
44. **Mistrikova, J., and D. Blaskovic.** 1985. Ecology of the murine alphaherpesvirus and its isolation from lungs of rodents in cell culture. Acta Virol. **29:**312–317.
45. **Moorman, N. J., D. O. Willer, and S. H. Speck.** 2003. The gammaherpesvirus 68 latency-associated nuclear antigen homolog is critical for the establishment of splenic latency. J. Virol. **77:**10295–10303.
46. **Obar, J. J., D. C. Donovan, S. G. Crist, O. Silvia, J. P. Stewart, and E. J. Usherwood.** 2004. T-cell responses to the M3 immune evasion protein of murid gammaherpesvirus 68 are partially protective and induced with lytic antigen kinetics. J. Virol. **78:**10829–10832.
47. **Qunibi, W., O. Al-Furayh, K. Almeshari, S. F. Lin, R. Sun, L. Heston, D. Ross, M. Rigsby, and G. Miller.** 1998. Serologic association of human herpesvirus eight with posttransplant Kaposi's sarcoma in Saudi Arabia. Transplantation **65:**583–585.
48. **Rickabaugh, T. M., H. J. Brown, D. Martinez-Guzman, T. T. Wu, L. Tong, F. Yu, S. Cole, and R. Sun.** 2004. Generation of a latency-deficient gammaherpesvirus that is protective against secondary infection. J. Virol. **78:**9215–9223.
49. **Rickinson, A. B., and E. Kieff.** 2001. Epstein-Barr virus, p. 2575–2628. *In* D. M. Knipe and P. M. Howley (ed.), Fields virology, 4th ed., vol. 2. Lippincott/The Williams & Wilkins Co., Philadelphia, PA.
50. **Roy, D. J., B. C. Ebrahimi, B. M. Dutia, A. A. Nash, and J. P. Stewart.** 2000. Murine gammaherpesvirus M11 gene product inhibits apoptosis and is expressed during virus persistence. Arch. Virol. **145:**2411–2420.
51. **Sarid, R., O. Flore, R. A. Bohenzky, Y. Chang, and P. S. Moore.** 1998. Transcription mapping of the Kaposi's sarcoma-associated herpesvirus (human herpesvirus 8) genome in a body cavity-based lymphoma cell line (BC-1). J. Virol. **72:**1005–1012.
52. **Smith, G. A., and L. W. Enquist.** 1999. Construction and transposon mutagenesis in *Escherichia coli* of a full-length infectious clone of pseudorabies virus, an alphaherpesvirus. J. Virol. **73:**6405–6414.
53. **Soulier, J., L. Grollet, E. Oksenhendler, P. Cacoub, D. Cazals-Hatem, P. Babinet, M. F. d'Agay, J. P. Clauvel, M. Raphael, L. Degos, et al.** 1995. Kaposi's sarcoma-associated herpesvirus-like DNA sequences in multicentric Castleman's disease. Blood **86:**1276–1280.
54. **Stevenson, P. G., G. T. Belz, J. D. Altman, and P. C. Doherty.** 1999. Changing patterns of dominance in the $CD8^+$ T-cell response during acute and persistent murine gamma-herpesvirus infection. Eur. J. Immunol. **29:**1059–1067.
55. **Stevenson, P. G., G. T. Belz, M. R. Castrucci, J. D. Altman, and P. C. Doherty.** 1999. A gamma-herpesvirus sneaks through a $CD8^+$ T-cell response primed to a lytic-phase epitope. Proc. Natl. Acad. Sci. U. S. A. **96:**9281–9286.
56. **Stevenson, P. G., J. S. May, X. G. Smith, S. Marques, H. Adler, U. H. Koszinowski, J. P. Simas, and S. Efstathiou.** 2002. K3-mediated evasion of $CD8^+$ T cells aids amplification of a latent gamma-herpesvirus. Nat. Immunol. **3:**733–740.
57. **Stewart, J. P., N. Micali, E. J. Usherwood, L. Bonina, and A. A. Nash.** 1999. Murine gamma-herpesvirus 68 glycoprotein 150 protects against virus-induced mononucleosis: a model system for gammaherpesvirus vaccination. Vaccine **17:**152–157.
58. **Stewart, J. P., E. J. Usherwood, A. Ross, H. Dyson, and T. Nash.** 1998. Lung epithelial cells are a major site of murine gammaherpesvirus persistence. J. Exp. Med. **187:**1941–1951.
59. **Sun, R., S. F. Lin, L. Gradoville, Y. Yuan, F. Zhu, and G. Miller.** 1998. A viral gene that activates lytic cycle expression of Kaposi's sarcoma-associated herpesvirus. Proc. Natl. Acad. Sci. U. S. A. **95:**10866–10871.
60. **Sunil-Chandra, N. P., S. Efstathiou, and A. A. Nash.** 1992. Murine gammaherpesvirus 68 establishes a latent infection in mouse B lymphocytes in vivo. J. Gen. Virol. **73:**3275–3279.
61. **Swanton, C., D. J. Mann, B. Fleckenstein, F. Neipel, G. Peters, and N. Jones.** 1997. Herpes viral cyclin/Cdk6 complexes evade inhibition by CDK inhibitor proteins. Nature **390:**184–187.
62. **Terry, L. A., J. P. Stewart, A. A. Nash, and J. K. Fazakerley.** 2000. Murine gammaherpesvirus-68 infection of and persistence in the central nervous system. J. Gen. Virol. **81:**2635–2643.
63. **Tibbetts, S. A., J. S. McClellan, S. Gangappa, S. H. Speck, and H. W. T. Virgin.** 2003. Effective vaccination against long-term gammaherpesvirus latency. J. Virol. **77:**2522–2529.
64. **Usherwood, E. J., A. J. Ross, D. J. Allen, and A. A. Nash.** 1996. Murine gammaherpesvirus-induced splenomegaly: a critical role for CD4 T cells. J. Gen. Virol. **77:**627–630.
65. **Usherwood, E. J., K. A. Ward, M. A. Blackman, J. P. Stewart, and D. L. Woodland.** 2001. Latent antigen vaccination in a model gammaherpesvirus infection. J. Virol. **75:**8283–8288.

66. **van Dyk, L. F., J. L. Hess, J. D. Katz, M. Jacoby, S. H. Speck, and H. I. Virgin.** 1999. The murine gammaherpesvirus 68 v-cyclin gene is an oncogene that promotes cell cycle progression in primary lymphocytes. J. Virol. **73:**5110–5122.
67. **van Dyk, L. F., H. W. T. Virgin, and S. H. Speck.** 2000. The murine gammaherpesvirus 68 v-cyclin is a critical regulator of reactivation from latency. J. Virol. **74:**7451–7461.
68. **Virgin, H. W. T., P. Latreille, P. Wamsley, K. Hallsworth, K. E. Weck, A. J. Dal Canto, and S. H. Speck.** 1997. Complete sequence and genomic analysis of murine gammaherpesvirus 68. J. Virol. **71:**5894–5904.
69. **Virgin, H. W. T., R. M. Presti, X. Y. Li, C. Liu, and S. H. Speck.** 1999. Three distinct regions of the murine gammaherpesvirus 68 genome are transcriptionally active in latently infected mice. J. Virol. **73:**2321–2332.
70. **Weck, K. E., M. L. Barkon, L. I. Yoo, S. H. Speck, and H. I. Virgin.** 1996. Mature B cells are required for acute splenic infection, but not for establishment of latency, by murine gammaherpesvirus 68. J. Virol. **70:**6775–6780.
71. **Wherry, E. J., and R. Ahmed.** 2004. Memory CD8 T-cell differentiation during viral infection. J. Virol. **78:**5535–5545.
72. **Wherry, E. J., D. L. Barber, S. M. Kaech, J. N. Blattman, and R. Ahmed.** 2004. Antigen-independent memory CD8 T cells do not develop during chronic viral infection. Proc. Natl. Acad. Sci. U. S. A. **101:**16004–16009.
73. **Woodland, D. L., E. J. Usherwood, L. Liu, E. Flano, I. J. Kim, and M. A. Blackman.** 2001. Vaccination against murine gamma-herpesvirus infection. Viral Immunol. **14:**217–226.
74. **Wu, T. T., L. Tong, T. Rickabaugh, S. Speck, and R. Sun.** 2001. Function of Rta is essential for lytic replication of murine gammaherpesvirus 68. J. Virol. **75:**9262–9273.
75. **Wu, T. T., E. J. Usherwood, J. P. Stewart, A. A. Nash, and R. Sun.** 2000. Rta of murine gammaherpesvirus 68 reactivates the complete lytic cycle from latency. J. Virol. **74:**3659–3667.